

C_2 -Symmetric Dibenzosuberane-Based Helicenes as Potential Chirochromic Optical Switches

Chien-Tien Chen* and Y-Chen Chou

Contribution from the Department of Chemistry, National Taiwan Normal University, Taipei, Taiwan, R.O.C.

Received September 13, 1999. Revised Manuscript Received May 31, 2000

Abstract: Three C_2 -symmetric (10*R*,11*R*)-diethyl substituted dibenzosuberane (DBS)-based helicenes with varying steric and conjugation demands of their bottom fragments were synthesized. The X-ray analyses of their precursors-episulfides reveal the preferred conformation of the DBS skeleton possessing equatorially oriented ethyl groups at C-8 and C-9 positions. In all cases, the absolute configuration in the episulfide moiety is *S*, which can lead stereospecifically to the corresponding *P* helicenes after the reductive desulfurization of the episulfides. Only the helicene-**7a** with the bottom part derived from α -tetralone was found photoswitchable in reasonable time scale. Photoisomerization of the diastereomerically pure (10*R*,11*R*,*P*)-helicene (**7a**) at 280 nm led to virtually exclusive formation of the opposite *M* form-diastereomer **7a'** (**7a'**/**7a** = 99.6/0.4). The preferential return of **7a'** to **7a** can be effected upon irradiation at 254 nm (**7a'**/**7a** = 33/67) or thermally at 130 °C (**7a'**/**7a** = 0/100). The photoinduced switching process amounts to a 133% difference in de (from 99.2% to -34%). The concomitant change of helicene chirality between these two diastereomeric photostationary states augurs well for their potential application as an optical switch in LC materials. To our knowledge, our system serves as the best chirochromic optical switch as compared to the examples possessing similar photochromic properties.

Liquid crystalline (LC) materials are consisted of relatively flat or bar-like molecules whose alignments can be modulated by electric and/or magnetic fields. It has been well recognized that a common nematic LC phase with rough alignment along one direction can be induced to a twisted nematic (i.e., cholesteric) one with helical continuum lacking layer boundaries by the action of a LC-like chiral dopant, Figure 1.¹ More importantly, the enantiomeric chiral additives can effect the corresponding cholesteric phases of opposite helical handedness. In principle, a pair of enantiomeric molecules with bistability that can be interconverted reversibly by an external mediator may be utilized as a LC-based memory unit with binary logic.² Unfortunately, the interchange of stereogenic, enantiomeric molecules requires bond-breaking and bond-forming events. Nevertheless, axially dissymmetric helicenes constitute one major category of organic compounds meeting this requirement due to their susceptibility to interchange by light.³ So far, there are two main approaches to realize such contentions. The first one involves photoresolution of enantiomeric helicenes^{4,5} by

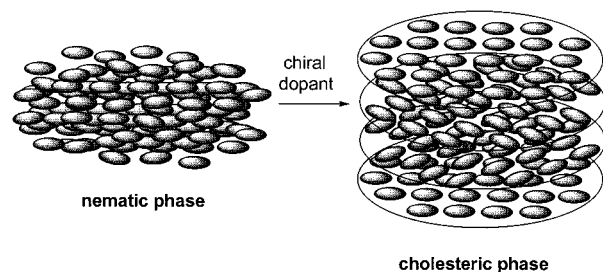


Figure 1. Phase change from a nematic to a cholesteric one under the influence of a chiral additive.

circularly polarized lights (approach I, Scheme 1). Research endeavors toward this aspect has reached a preliminary success despite the concentration of the helicene dopants could not be reduced to a reasonable level (e.g., 1–5 wt %). Therefore, it would not be practical for them to be used as LC-based optical switches unless helicenes exhibiting higher ee_{ps} ⁶ or twisting powers can be accessed. The second approach is to transform the enantiomeric helicenes into the corresponding geometrical (diastereomeric) ones by incorporating different substituents onto each geminal aromatic ring, Scheme 1.⁷ Despite a preliminary report by Feringa and co-workers in 1991 using thioxanthene-based helicenes exhibited a limited modulation behavior (from +36% de to +28% de), a promising optical switch was subsequently realized on similar helicenes with a donor-acceptor pairing system.⁸ High switching selectivities of 10/90 and 70/30 (*P*/*M'*) were achieved (+40% de to -80% de).⁹

(1) Solladié, G.; Zimmermann, R. G. *Angew. Chem., Int. Ed. Engl.* **1984**, *23*, 348.

(2) Feringa, B. L.; Jager, W. F.; de Lange, B. *Tetrahedron* **1993**, *49*, 8267.

(3) (a) Feringa, B. L.; van Delden, R. A. *Angew. Chem., Int. Ed.* **1999**, *38*, 3418. (b) For a review of asymmetric photochemistry in solution, see: Rau, H. *Chem. Rev.* **1983**, *83*, 535.

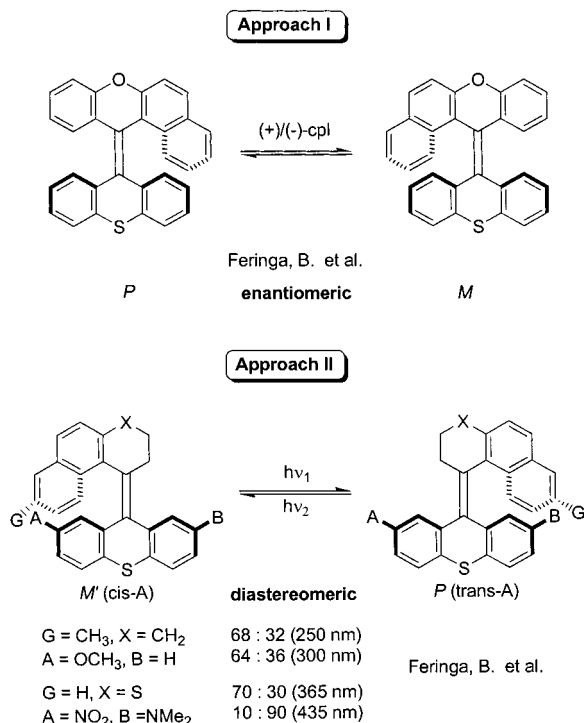
(4) (a) Udayakumar, B. S.; Schuster, G. B. *J. Org. Chem.* **1993**, *58*, 4165. (b) Huck, N. P.; Jager, W. F.; de Lange, B.; Feringa, B. L. *Science* **1996**, *273*, 1686.

(5) For the photoresolution of molecules with axial chirality, see: (a) Lemieux, R. P.; Schuster, G. B. *J. Org. Chem.* **1993**, *58*, 100. (b) Zhang, M.; Schuster, G. B. *J. Phys. Chem.* **1992**, *96*, 3063. (c) Zhang, Y.; Schuster, G. B. *J. Org. Chem.* **1995**, *60*, 7192. (d) Suarez, M.; Schuster, G. B. *J. Am. Chem. Soc.* **1995**, *117*, 6732. (e) Burnham, K. S.; Schuster, G. B. *J. Am. Chem. Soc.* **1999**, *121*, 10245. (f) see also: Li, J.; Schuster, G. B.; Cheon, K.-S.; Green, M. M.; Selinger, J. V. *J. Am. Chem. Soc.* **2000**, *122*, 2603.

(6) ee_{ps} stands for the enantiomeric excess of a helicene under a photostationary state at a given irradiation wavelength.

(7) (a) Huck, N. P. M.; Feringa, B. L. *J. Chem. Soc., Chem. Commun.* **1995**, 1095. (b) Feringa, B. L.; Jager, W. F.; de Lange, B. *J. Chem. Soc., Chem. Commun.* **1993**, 288. (c) Feringa, B. L.; Jager, W. F.; de Lange, B.; Meijer, E. W. *J. Am. Chem. Soc.* **1991**, *113*, 5468.

Scheme 1



As an extension of an ongoing program centered on the use of C_2 -symmetric dibenzosuberanes (DBS) as chiral templates in asymmetric catalysis,¹⁰ we have been recently engaged in assessing the feasibility of incorporating our templates into the helicenes on the basis of two considerations. First, the central seven-membered ring in DBS makes the flanking aryl rings in closer contact with that (or those) in the other end of the central double bond. Due to the increasing steric encumbrance around the central double bond, the energy barrier to thermal racemization (or epimerization) for the DBS-based helicenes may be significantly increased,¹¹ Scheme 2. Second, desymmetrization of the enantiomeric helicenes but still maintaining the enantiomeric relationship of the helicene chirality can be achieved by installing a C_2 chirality in the DBS backbone (approach II, Scheme 2). Under such circumstances, a chirochromic optical switch may be attained if two photostationary states of opposite diastereomeric preferences can be reached by photoisomerization. Intrigued by the seminal study of Schuster on the chirochromic phototriggers derived from BINOL-based diastereomeric acetals,¹² we sought to examine the switching profiles of our C_2 -symmetric DBS-based helicenes. We herein describe our results toward this approach.

Results and Discussions

Synthesis of (10*R*,11*R*)-Diethyl-dibenzosuberone 4. Platzek and Snatzke have reported the synthesis of C_2 -symmetric diol-

(8) (a) Jager, W. F.; de Jong, J. C.; de Lange, B.; Huck, N. P. M.; Meetsma, A.; Feringa, B. L. *Angew. Chem., Int. Ed. Engl.* **1995**, *34*, 348. (b) Feringa, B. L.; Huck, N. P. M.; van Doren, H. A. *J. Am. Chem. Soc.* **1995**, *117*, 9927.

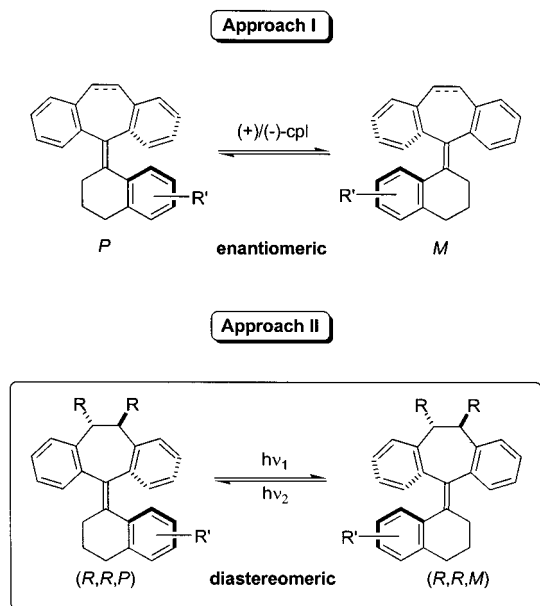
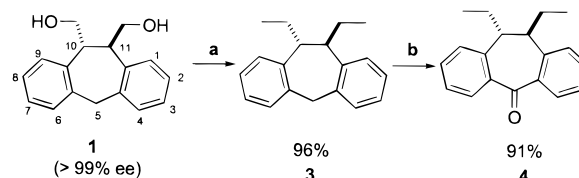
(9) For reviews, see: (a) Feringa, B. L.; Huck, N. P. M.; Schoevarrs, A. M. *Adv. Mater.* **1996**, *8*, 681. (b) Feringa, B. L.; van Delden, R. A.; Koumura, N.; Geertsema, E. M. *Chem Rev.* **2000**, in press.

(10) (a) Chen, C.-T.; Chao, S.-D.; Yen, K.-C.; Chen, C.-H.; Chou, I.-C.; Hon, S.-W. *J. Am. Chem. Soc.* **1997**, *119*, 11341. (b) Chen, C.-T.; Chao, S.-D.; Yen, K.-C. *Synlett* **1998**, 924. (c) Chen, C.-T.; Chao, S.-D. *J. Org. Chem.* **1999**, *64*, 1090.

(11) A barrier of 32 kcal/mol to racemization for tribenzocycloheptatriene-based helicenes has been documented: Tochtermann, W.; Küppers, H.; Franke, C. *Chem Ber.* **1968**, *101*, 3808.

(12) For the definition of a chirochromic optical switch and its realization, see: Zhang, M.; Schuster, G. B. *J. Am. Chem. Soc.* **1994**, *116*, 4852.

Scheme 2

Scheme 3^a

^a (a) (i) TsCl/Et₃N/CH₂Cl₂, cat. DMAP, (ii) Me₂CuLi/ether, -10 °C; (b) KMnO₄, dicyclohexano-18-crown-6, benzene.

1, a common skeleton in various antiinflammatory drugs, in scalemic form.¹³ This resolved (10*R*,11*R*)-**1** was utilized as a conceivable (10*R*,11*R*)-diethyl-dibenzosuberone precursor, whose enantiomeric purity was determined to be >99% ee by HPLC analysis on a chiral column (Chiralcel OJ), Scheme 3. To derivatize the alcohol moieties into the corresponding ethyl appendages, the diol-**1** was tosylated smoothly in 96% yield with *p*-toluenesulfonyl chloride (TsCl) in CH₂Cl₂ in the presence of Et₃N and catalytic 4-*N,N*-(dimethylamino)pyridine. Double S_N2 displacement of the ditosylate **2** with (CH₃)₂CuLi at -10 °C provided the diethyl-DBS **3** quantitatively.¹⁴ It should be noted that the displacement reaction needs to be carried out in pure ether despite the poor solubility of **2** in this solvent. Similar reaction conditions in THF led to complete recovery of the starting ditosylate **2**. The C5-methylene flanked by the dibenzo unit in **3** was readily oxidized at ambient temperature to the corresponding ketone-**4** in 91% yield by KMnO₄ (2.5 equiv) in benzene using dicyclohexano-18-crown-6 as a phase transfer catalyst.¹⁵

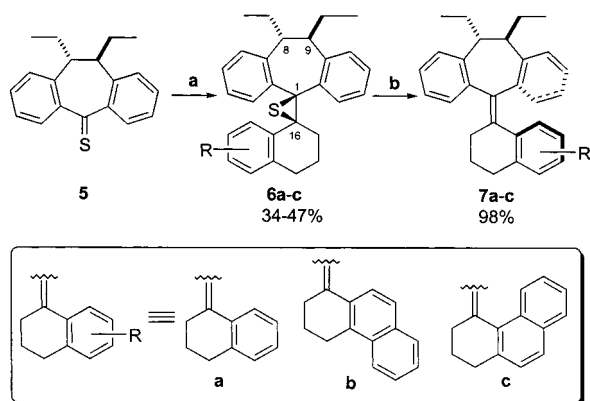
Synthesis of (10*R*,11*R*)-Diethyl-DBS-based Helicenes 7a-c. By following a helicene assembly protocol similar to Feringa's,¹⁶ we have synthesized the desired triarylethylene-type helicenes by employing (10*R*,11*R*)-diethyl-DBS-5-thione **5** and three different diazo fragments with varying degrees of conjugation and steric congestion (i.e., **a**-mono, **b**-exo, and **c**-endo), Scheme 4. The requisite thioketone **5** can be readily

(13) Platzek, J.; Snatzke, G. *Tetrahedron* **1987**, *43*, 4947 and references therein.

(14) Posner G. H. *Org. React.* **1975**, *22*, 253.

(15) Sam, D. J.; Simmons, H. E. *J. Am. Chem. Soc.* **1972**, *94*, 4024.

(16) de Lange, B.; Jager, W. F.; Feringa, B. L. *Mol. Cryst. Liq. Cryst.* **1992**, *217*, 127.

Scheme 4^a

^a (a) Hydrazone, Ag₂O/MgSO₄, KOH/MeOH, CH₂Cl₂, -30 → 0 °C; (b) Cu/xylylene, reflux or HMPT/CH₂Cl₂.

generated by thiation of the corresponding ketone **4** with P₄S₁₀ or Lawesson's reagent.¹⁷ The thioketone-**5** is moisture sensitive and tends to hydrolyze with time even at -20 °C. Therefore, it had better be prepared and used immediately after purification. Cycloaddition of the appropriately in situ-generated diazo compounds arising from α-tetralone- and dihydrophenanthrenone-derived hydrazones¹⁸ with thioketone-**5** in a 1,3-dipolar fashion and subsequent extrusion of molecular nitrogen led to episulfides **6a-c** in moderate yields (34–47%).^{19a} It should be noted that all three episulfides were furnished as single diastereomers as evidenced by HPLC analyses of the crude products on chiral columns (Chiralcel AD and Chiralpak OT). Reductive desulfurization of the thirranes **6a-c** by Cu powder in refluxing xylene or by HMPT²⁰ at ambient temperature led to the respective dissymmetric helicenes **7a-c** in essentially quantitative yields (98%).

Absolute Stereochemistry of Episulfides 6a-c and Helicenes 7a-c. In all instances, the structural identities and absolute stereochemistry of episulfides **6a-c** were conformed by X-ray crystallographic analyses, Figure 2. Several important structural characteristics are summarized as follows: (1) The DBS skeleton adopts a butterfly shape and both the ethyl groups are positioned equatorially with the central seven-membered ring in a chairlike conformation. (2) The central thirrane ring is slightly twisted by 2–3° for the left dihedral angle (ϕ_1) in **6a** and **6b**, Table 1. This distortion is significantly larger (10.6°) in the endo-**6c** presumably due to the increasing steric encumbrance of the endo-naphthyl unit. The larger distortion with concomitant release of eclipsed interactions around the episulfide unit might be responsible for the larger dihedral angle (51.2°) observed between the aryl ring A and ring C in **6c**. On the other hand, the right dihedral angles (ϕ_2) around the episulfide units are in the range of 4–8.2° with those in **6b** and **6c** being slightly larger than that in **6a** (3.9°). Therefore, the steric demand of the ring C modulates the aryl torsions of both rings A and B. (3) In all three cases, both bond angles (α and α') remain essentially constant with α' uniformly larger by 8–10°. (4) The aryl ring C in the lower fragment is placed syn to the proximal equatorial

(17) (a) Safarzadeh-Amiri, A.; Verrall, R. E.; Steer, R. P. *Can. J. Chem.* **1983**, *61*, 894. (b) Cherkasov, R. A.; Kutyrev, G. A.; Pudovik, A. N. *Tetrahedron* **1985**, *41*, 2567. (c) Mayer, R. *Chem. Ber.* **1957**, *90*, 2.

(18) (a) Newkome, G. R.; Fishel, D. L. *J. Chem. Soc.* **1966**, *31*, 677. (b) Osterodt, J.; Nieger, M.; Windscheif, P.-M.; Vögtle, F. *Chem. Ber.* **1993**, *126*, 6, 2331.

(19) (a) Their chemical yields were all = 80% if based on recovered **1**. (b) See the Supporting Information for the X-ray data of **6a-c** and **7c**.

(20) (a) Neureiter, N. P.; Bordwell, F. G. *J. Chem. Soc.* **1959**, *81*, 578. (b) Buynak, J. D.; Graff, N. M.; Jadhav, K. P. *J. Org. Chem.* **1984**, *49*, 1828.

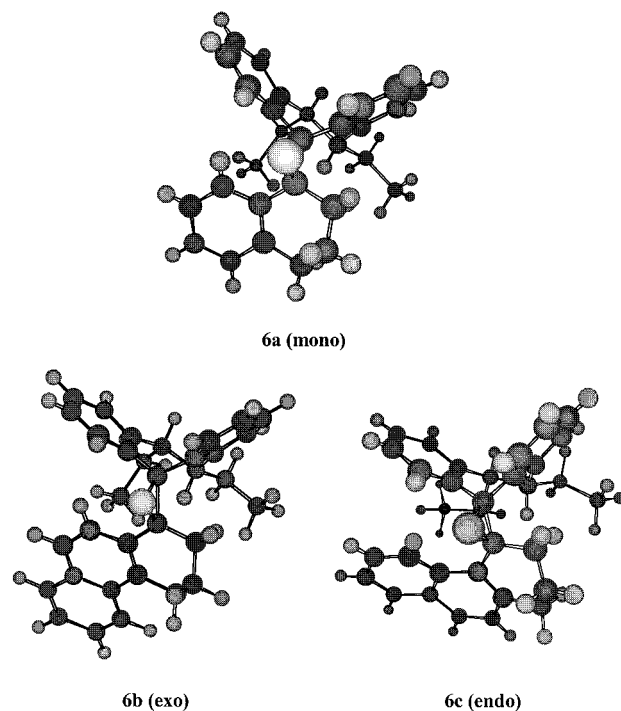
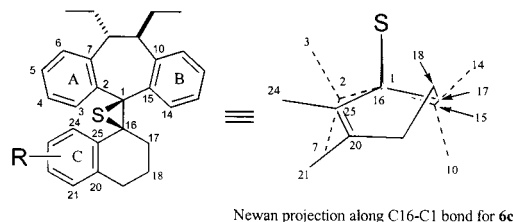


Figure 2. Chem-3D Presentations for X-ray Structures of **6a-c**.

Table 1. Selected Dihedral Angles, ϕ (degrees), and Bond Angles, α and α' (degrees), from the X-ray Structures of **6a-c**



Newman projection along C16-C1 bond for **6c**

	mono- 6a	exo- 6b	endo- 6c
ϕ_1 (C25–C16–C1–C2) ^a	-2.0	3.0	10.6
ϕ_2 (C17–C16–C1–C15)	3.9	7.1	8.2
ϕ_3 (C24–C25–C2–C3)	41.2	41.2	51.2
α (C2–C1–C15)	106.3	107.6	105
α' (C25–C16–C7)	115.4	115.5	115.3

^a For clarity, the numberings consistent with those in the X-ray structure for **6a** are adopted.

ethyl group even in the endo-naphthyl case **6c**.^{19b} This conformational preference may have to do with the crystal packing effect since an opposite conformational preference (i.e., with ring C syn to the proximal axial hydrogen) was found in the achiral, parent system; (5) The absolute configuration of the episulfide moiety in **6a-c** (Figure 2) was determined to be *S* at C16,²¹ which would lead to a *P* chirality in the resultant helicenes **7a-c** as inferred by the crystal structure of the endo helicene-**7c** (vide infra).^{19b} The absolute *S* stereo-control in **6a-c** implies an exclusive approach of the thioketone **5** from the *si* face of the respective diazo compound, by which the aryl ring in the diazo compound stays away from the proximal and distal axial hydrogens at C8 and C9 in **5**.

So far, single crystals suitable for X-ray diffraction analysis were available only for the endo-helicene **7c**, Figure 3. The structure of the helicene **7c** shares a couple of the common

(21) The newly created stereocenter is carbon-16. Carbon-1 in **6a-c** is not a stereocenter since it is located in a C₂ axis in the common starting material-thioketone **5**.

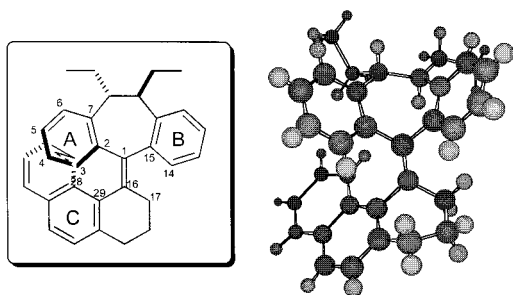


Figure 3. Chem 3D Presentation of the X-ray Structure of **7c**.

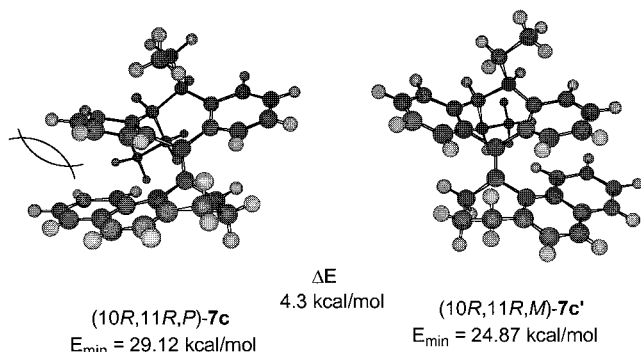


Figure 4. Chem-3D Presentations of Calculated Structures for $(10R,11R,P)\text{-7c}$ and $(10R,11R,M)\text{-7c}'$.

characteristics with those of the episulfides **6a–c**. Namely, the DBS skeleton adopts a butterfly shape and both the ethyl groups are positioned equatorially with the central seven-membered ring in a chairlike conformation. The aryl C ring in **7c** is also placed syn to the proximal equatorial ethyl group. Similar conformational preference (i.e., with C ring syn to the proximal equatorial hydrogen) was also observed in the achiral, parent systems.²² The preferential equatorial disposition of the ethyl groups in the helicene-**7c** is in harmony with its helicene chirality beside a possible crystal packing effect (vide infra). In the molecular simulation of $(10R,11R)\text{-7c}$ the ethyl groups were predicted to be placed axially in order to prevent the repulsive gauche-butane interaction between the ethyl groups, Figure 4.²³ Under such circumstances, the $(10R,11R,M)\text{-7c}'$ was shown to be more stable than $(10R,11R,P)\text{-7c}$ by 4.3 kcal/mol in view of the severe steric interaction between the endo-naphthyl ring and the proximal axial ethyl group. Therefore, we surmise that $(10R,11R)$ -diethyl-DBS-based helicenes with *M* chirality would prefer to have a DBS conformation with axially oriented ethyl groups. On the other hand, the helicenes with *P* chirality call for an opposite DBS conformation with equatorial ethyl groups as evidenced by the X-ray crystal structure of **7c**.

As revealed in the X-ray structure of **7c** (Figure 3), there is a small deviation of planarity around the central olefin unit ($\sim 2^\circ$). The phenyl torsional angle between the A ring and the central double bond is 52.5° and that between the B ring and the central double bond is 63.5° , which are also observed in all the achiral parent helicenes.²² Apparently, the ethyl groups in **7c** do not impose any significant torsional strain onto the DBS template. On the other hand, the dihedral angle between the C ring and the central double bond is 61.2° . This angle is 9° larger than that of the corresponding achiral endo-helicene and is increased by 28° as compared to that of the model mono-helicene (33.1°). Apparently, the larger dihedral angle serves

to accommodate the steric congestion around the helical turn (i.e., between the endo-naphthyl ring and the A ring in DBS). Finally, the absolute helicene chirality of **7c** is *P* which corresponds to a stereospecific chirality transfer from the $(10R,11R,S)$ -episulfide-**6c**. On the bases of (1) the unambiguous structural determinations of **6a–c** and **7c**, (2) the stereospecific chirality transfer from the episulfides to the corresponding helicenes, and (3) same exciton chirality observed in circular dichroism (CD) spectra for **7a–c**,^{22,24} we can conclude that **7a–c** all possess the same absolute helicene chirality-*P*.

Photochemistry of Helicenes 7a–c. To judiciously choose irradiation wavelengths to effect photochemical shuttling between diastereomeric helicenes, both their UV–vis spectra with fully calibrated extinction coefficients (ϵ) are required. One can easily assess their relative abundances under the pss at a certain irradiation wavelength by their given ϵ . The isomeric excess of the pss from irradiation at a given wavelength is given by: $[\text{de}]_{\text{pss}} = (\mathbf{7a} - \mathbf{7a}')/(\mathbf{7a} + \mathbf{7a}') = [(\epsilon_{7a'}\Phi_{7a'-7a} - \epsilon_{7a}\Phi_{7a-7a'})/(\epsilon_{7a}\Phi_{7a'-7a} + \epsilon_{7a'}\Phi_{7a-7a'})]$. The extinction coefficient difference between the diastereomers at a given wavelength can directly reflect the $[\text{de}]_{\text{pss}}$ as long as the photoisomerization quantum yields ($\Phi_{7a'-7a}$ and $\Phi_{7a-7a'}$) for both processes stay similar. That is to say, to effect efficient switching between them in a highly selective manner (e.g., $>90/10$), irradiations are better targeted at regions with significant changes in extinction coefficients. At the onset, photoisomerization by irradiations at 260 and 300 nm was randomly selected for $(10R,11R,P)\text{-7a}$ due to lack of any UV spectrum information for the corresponding diastereomer $(10R,11R,M)\text{-7a}'$, which was unavailable by chemical synthesis but subsequently obtained by photoisomerization at 280 nm (vide infra). Both experiments^{25a} were conducted in degassed hexane and were monitored both by CD spectroscopy and HPLC analysis on Chiralpak OT until constant compositions (i.e., under photostationary states; pss) were reached (up to 3 h). In both experiments, preferential formation of the opposite **7a'** was observed (**7a'**/**7a** = 56/44 and 67/33, respectively). By subtracting the UV spectrum of the diastereomeric helicenes with a 67/33 (**7a'**/**7a**) composition from that of the pure **7a**, we were able to locate a couple of other wavelengths (250 and 290 nm) with distinct difference in extinction coefficients from the difference spectrum. Photoisomerization of **7a** near these two irradiation wavelengths (254^{25b} and 280 nm^{25a}) led to two new pss with complementary diastereoselectivities of 33/67 and 99.6/0.4 (**7a'**/**7a**), respectively. Figure 5 shows a stacked plot of CD spectra for monitoring the photoisomerization of **7a** at 280 nm with time. As revealed in the plot, there are two isodichroic points²⁶ at 214 and 271 nm, respectively. Their presence strongly indicates the newly generated product (**7a'**) is the only homogeneous product in solution and has similar photochromic properties as in **7a**. The diastereomeric identity of **7a'** relative to **7a** was further secured by two independent lines of evidences. First, the opposite sign of the Cotton effects in the range of 239 to 264 nm suggests a helicene chirality reversal for **7a'**. Second, a complete return of **7a'** to **7a** can be effected upon heating a solution of **7a'** in xylene at 130°C for 2 h. The

(24) Harada, N.; Nakanishi, K. *Circular Dichroic Spectroscopy: Exciton Coupling in Organic Photochemistry*; University Science Books: Mill Valley, CA, 1983.

(25) (a) Irradiations were carried out with a 300 W Xe lamp equipped with a monochromator with a slit size equivalent to 16 nm bandwidth. (b) Irradiation was performed with a 100 W Hg lamp equipped with a 20-nm bandwidth filter.

(26) For a recent example on using the presence of isodichroic points in CD spectra to support structure similarities of several oligo(phenylene ethynylene)s, see: Gin, M. S.; Yokozawa, T.; Prince, R. B.; Moore, J. S. *J. Am. Chem. Soc.* **1999**, *121*, 2643.

(22) Unpublished results from this laboratory.

(23) Molecular modeling was carried out on an SGI–Indy Worksystem. Global minimum conformations of the diastereomeric pair, **7c** and **7c'**, were calculated with the Sybyl simulation package.

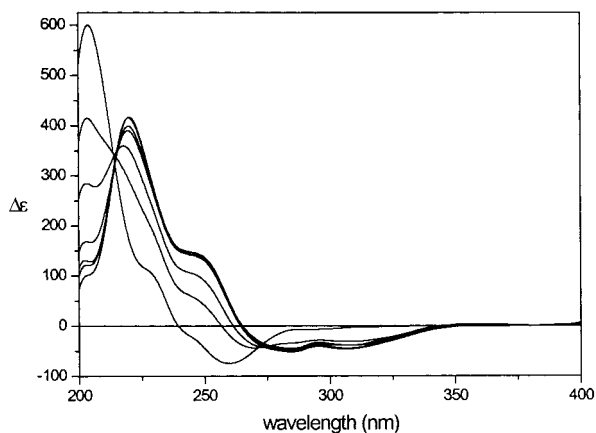


Figure 5. A stacked plot of CD spectra for the photoisomerization of **7a** in hexane irradiated at 280 nm with time.

Table 2. Diastereoselective Photoisomerization by Irradiation of (10*R*,11*R*,*P*)-**7a** in Different Solvents with Varying Wavelengths

entry	solvent	λ (nm) ^a	dr (7a : 7a') ^b	de, ^c %
1	hexane	254 ± 10 ^d	67:33	+34
2	hexane	260 ± 8	44:56	-12
3	hexane	280 ± 8	0.4:99.6	-99.2
4	hexane	300 ± 8	33:67	-34
5	hexane	310 ± 8	70:30	+40
6	hexane	330 ± 8	no change	
7	THF	254 ± 10	61:39	+22
8	THF	280 ± 8	7:93	-86
9	THF	310 ± 8	54:46	+8
10	cyclohexane	254 ± 10	79:21	+58
11	cyclohexane	280 ± 8	38:62	-24
12	cyclohexane	310 ± 8	82:18	+64
13	toluene	254 ± 10	46:54	-8
14	toluene	280 ± 8	9.5:90.5	-81
15	toluene	310 ± 8	61:39	+22

^a Irradiation time is 3 h unless otherwise stated. ^b Determined by HPLC analysis on Chiralpak OT column. ^c Defined as (**7a** - **7a'**)/(**7a** + **7a'**). ^d Irradiation time is 30 s.

structure of **7a'** was ultimately characterized by NMR and MS spectrometric means.

The interconversion between these two pss (at 280 and 254 nm) is modestly reversible with slight decomposition (due to free radical-mediated oxygenation reaction). On the other hand, the analogous exo- and endo-helicenes (**7b** and **7c**) are essentially photochemically inert. No appreciable changes in compositions were observed by irradiating **7b** and **7c** at several wavelengths for 3 h presumably due to larger dihedral angles and higher distortion between the central double bond and the bottom parts.²⁷ The results of several photoisomerization experiments for **7a** in various solvents are compiled in Table 2. Similar switching profiles were observed in hexane, toluene, and THF at 254 and 310 nm. The pss compositions are solvent dependent particularly at 280 nm. The selectivity dropped from 99.6/0.4 to 93/7 and 91/9, respectively, when **7a** was irradiated in THF and in toluene (entries 8 and 14). Dramatically reduced selectivity (62/38, **7a'**/**7a**) was resulted in cyclohexane. However, more promising and opposite switching selectivities were found at 254 (21/79) and 310 nm (18/82, **7a'**/**7a**) in this solvent.

With the essentially diastereomerically pure **7a'** in hand (from the experiment in entry 3), we were able to take a closer look

(27) The endo helicene-**7c** exhibits very intriguing photophysical behaviors. A large increase in Stokes shift (50 nm) with a purplish-blue light ($\lambda = 430$ nm) emitting character and a 250-fold increase in Φ_f were observed uniquely for **7c**. Chen, C.-T.; Chang, I.-J.; Chou, Y.-C.; Kao, J.-I.; Lee, T.-W.; Lin, J.-S.; Lee, I.-J.; Wang, C.-L. Manuscript in preparation.

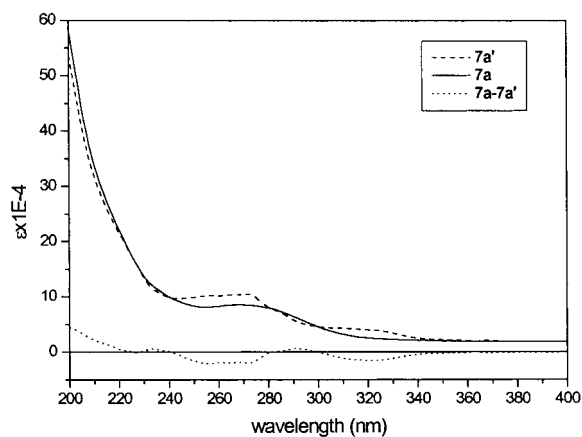


Figure 6. UV spectra of **7a** and **7a'** and the UV difference spectrum in hexane.

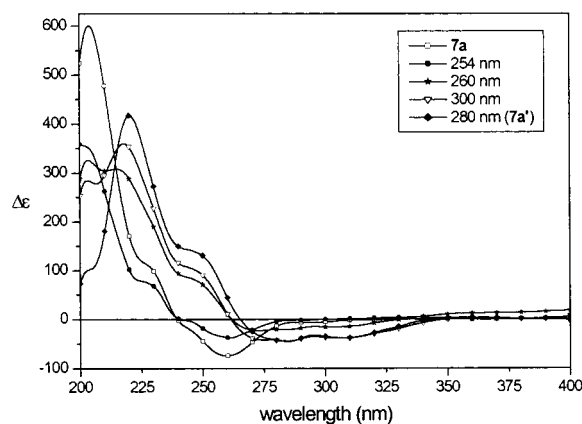


Figure 7. CD spectra of **7a** and the pss resulted from irradiation at 254, 260, 280, and 300 nm in hexane.

at its photophysical properties. As illustrated in the individual and difference UV spectra of **7a** and **7a'** in hexane, both isomers display very strong absorption around 200 nm and an intense absorption near 275 nm ($\epsilon = 80300$), Figure 6. Unlike **7a**, **7a'** exhibit much more unique absorptions at 255 and 325 nm. A significant increase in extinction coefficient in the latter absorption band (325 nm) in **7a'** suggests possible less phenyl distortions and thus better conjugation for the (10*R*,11*R*,*M*)-**7a'** diastereomer. As evidenced in the UV difference spectrum, well-defined extremes can be found at 230, 254, 273, 290, and 325 nm. Photoswitching of **7a** with irradiation wavelengths close to these extremes indeed led to distinctive pss and complementary pss particularly at 254 (or 310 nm) and 280 nm. Moreover, *the almost exclusive switching selectivity observed at 280 nm in hexane represents the most selective switching process to date by utilizing such a unfunctionalized helicene* (compared with the systems in approach II, Scheme 1).

Figure 7 shows the stacked CD spectra of helicene-**7a** and helicenes (**7a**/**7a'**) with diastereomeric compositions resulted from the experiments in hexane as compiled in Table 2 (entries 1–4). In marked contrast to Feringa's donor-acceptor-based helicenes,⁸ the CD spectra of **7a** and **7a'** displays opposite Cotton effects only around 239–264 nm. Nevertheless, CD still serves as a promising chiroptical technique for tracing the switching profiles of our helicenes by signs and by intensity differences. The significant changes in the CD spectra of **7a** and **7a'** as well as the 133% difference in de (i.e., from 99.2% to -34% de, entries 3 and 1) between two complementary pss make our helicenes potentially useful as an optical switch in LC materials.

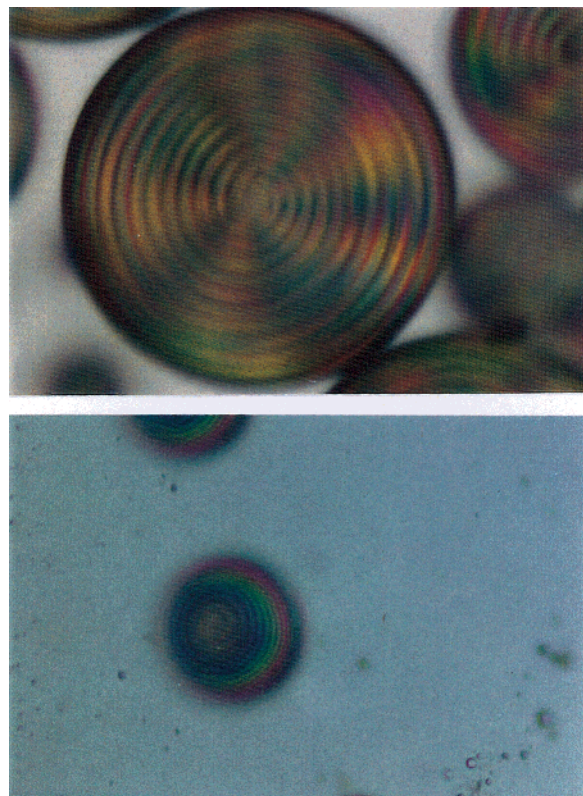


Figure 8. Droplets of K-15 containing (top) 1% (10R,11R,P)-**7a** (bottom) 1% (10R,11R,M)-**7a'** suspended in glycerol viewed at 200 \times magnification at room temperature. The distances between adjacent arms of the spiral are 133 μm and 50 μm , respectively.

We were so far unable to demonstrate the feasibility of **7a** as an optical switch in a UV transparent LC material like ZLI-1167^{28a} due to its poor solubility in ZLI-1167 at ambient temperature and the difficulty for determining the diastereomeric compositions after photoisomerization experiments.²⁹ Nevertheless, photoisomerization of **7a** in a 1:1 mixture of hexane and ZLI-1167 at 280 nm seems to display a similar diastereomeric preference as in pure cyclohexane, albeit with a longer irradiation time (5 h). Although the photoswitching selectivity for **7a** at 280 nm doped with LC materials such as ZLI-1167 and K-15^{28b} could not be determined, they would be expected to display similar switching profiles as in cyclohexane and toluene, respectively, in view of their similarity in core structures.

The helical twisting powers (β_M) of **7a** and **7a'** were determined by the droplet method³⁰ in a nematic LC K-15. As shown in Figure 8 (top), droplets of K-15 doped with 1% of **7a** suspended in glycerol were viewed microscopically at 200 \times magnification at ambient temperature. The helical pitch equals twice the distance between adjacent spirals. The pitch (p) of a cholesteric LC formed by addition of an optically active dopant to a nematic phase depends on its optical purity (γ), its helical twisting power (β_M), and its concentration (C , mol of dopant/mol of solution) according to $p = [\beta_M C \gamma]^{-1}$. This measurement provides a β_M value of 1.2 μm^{-1} ($p = 133 \mu\text{m}$) for **7a** in K-15. Similar measurement (bottom in Figure 8) for **7a'** (99.2% de) comes to a β_M value of 3.2 μm^{-1} ($p = 50 \mu\text{m}$).

(28) (a) ZLI-1167: 4-*n*-alkyl-4-cyano-1,1'-bicyclohexyls. (b) K-15: 4-cyano-4'-pentoxy-biphenyl.

(29) The retention time of ZLI-1167 happens to coincide with that of **7a** on HPLC chromatogram.

(30) (a) Seuron, P.; Solladie, G. *Mol. Cryst. Liq. Cryst.* **1979**, *56*, 1. (b) Candau, S.; LeRoy, P.; Debeauvais, F. *Mol. Cryst. Liq. Cryst.* **1973**, *23*, 283.

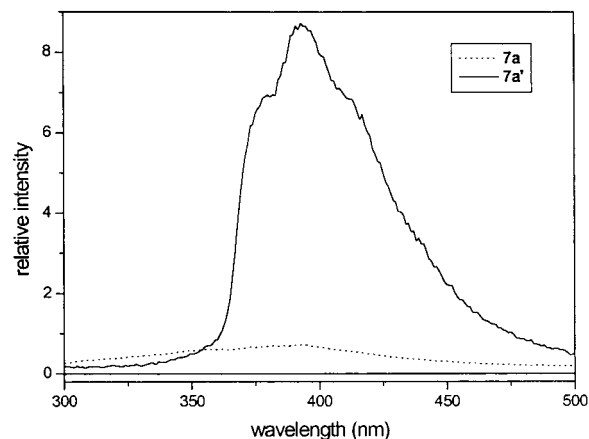


Figure 9. Emission spectra of helices **7a** and **7a'** in hexane.

The photochemical properties of the 10,11-diethyl-DBS-based helices resemble those of other arylethylenes such as stilbenes, triphenylethylenes, and tetraphenylethylenes. Their photophysical profiles have been examined theoretically and experimentally by steady-state and time-resolved spectroscopic means.³¹ The results indicated that the photoinduced isomerization involves delicate motions on the excited state potential energy surface imparted with at least three structurally well-defined states.³² Initial excitation of an arylethylene leads to a vertical (Franck–Condon) singlet state. Its torsional relaxation about the aryl-olefinic C–C bond furnishes a relaxed and emissive excited state (S_v). Subsequent rotation around the central olefinic C–C bond provides a nonemissive perpendicular (“phantom”) excited state (S_p). Internal relaxation of the phantom state to a perpendicular ground-state results in the final double bond isomerization. The extent of partition for S_p highly depends on the extent of coplanarity between the aryl and the olefinic moieties in S_v . The larger the coplanarity (or the smaller the torsional angle), the bigger the partition for S_p . Detailed photophysical analyses of the 10,11-diethyl-DBS-based helices are currently underway and it appears that the basic principles behind the photoinduced process are the same as they are for other arylethylenes.³³

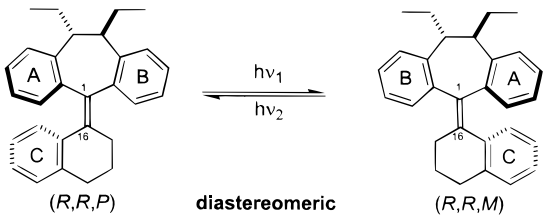
The extremely high switching selectivity of **7a** at 280 nm (except in cyclohexane) and the small difference in extinction coefficients between **7a** and **7a'** at 280 nm strongly suggest that there exists a preferential difference in photoisomerization quantum yields between $\Phi_{7a \rightarrow 7a'}$ and $\Phi_{7a' \rightarrow 7a}$. An indirect piece of evidence in support of this presumption is the observed large difference in fluorescence quantum yields between **7a** and **7a'** ($\Phi_{7a'}/\Phi_{7a} \approx 30$) at 280 nm in hexane (Figure 9).³⁴ Apparently, a lot more of the energy in the excited state of **7a'** is dissipated into fluorescent emission rather than double bond isomerization. To gain insights into the origin of the predominant photoisomerization efficiency of **7a**, molecular simulations of **7a** and

(31) (a) Pederson, S.; Banares, L.; Zewail, A. H. *J. Chem. Phys.* **1992**, *97*, 8801. (b) Satiel, J.; Sun, Y.-P. In *Photochromism: Molecules and Systems*; Durr, H.; Bouas-Laurent, H., Eds.; Elsevier: Amsterdam, 1990; p64. (c) Gegiou, D.; Muszkat, K. A.; Fischer, E. *J. Am. Chem. Soc.* **1968**, *90*, 13. (d) Schilling, C. L.; Hilinsky, E. F. *J. Am. Chem. Soc.* **1988**, *110*, 2296. (e) Shultz, D. A.; Fox, M. A. *J. Am. Chem. Soc.* **1989**, *111*, 6311. (f) Udayakumar, B. S.; Devados, C.; Schuster, G. B. *J. Phys. Chem.* **1993**, *97*, 8712 and references therein.

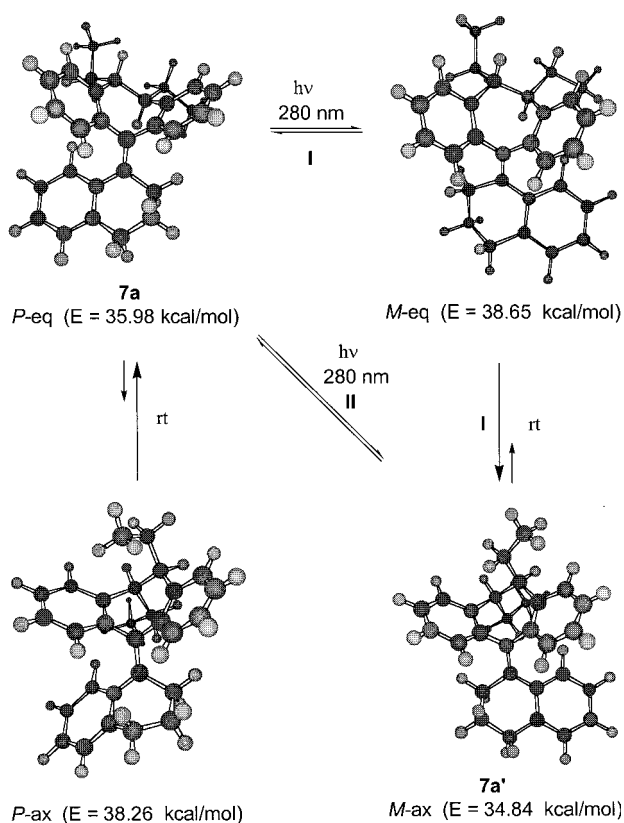
(32) (a) Zimmt, M. B. *Chem. Phys. Lett.* **1989**, *160*, 564. (b) Morais, J.; Ma, J.; Zimmt, M. B. *J. Phys. Chem.* **1991**, *95*, 3885. (c) Ma, J.; Zimmt, M. B. *J. Am. Chem. Soc.* **1992**, *114*, 9723.

(33) Chen, C.-T.; Chang, I.-J.; Chou, Y.-C.; Kao, J.-I.; Lee, T.-W.; Lin, J.-S.; Lee, I.-J.; Wang, C.-L. unpublished results from these laboratories.

(34) Huck, N. P. M.; Feringa, B. L. *J. Chem. Soc., Chem. Commun.* **1995**, 1095.

Table 3. Minimized Energies and Three Appropriate Phenyl Torsional Angles for **7a** and **7a'**


	7a		7a'	
	<i>P</i> -eq	<i>P</i> -ax	<i>M</i> -eq	<i>M</i> -ax
energy, kcal/mol	36.0	38.3	38.7	34.8
ϕ_1 (A and C1=C16)	61.9	69.3	-73.5	-55.4
ϕ_2 (B and C1=C16)	-79.3	-61.5	68.5	75.7
ϕ_3 (C and C16=C1)	39.3	38.1	-39.3	-39.6

Scheme 5

7a' with conformational permutations of the DBS were carried out both at the molecular mechanics (MM3) and the semi-empirical levels (PM3).³⁵ The minimized energies and three appropriate phenyl torsional angles for **7a** and **7a'** are compiled in Table 3. It should be noted that the DBS with the equatorially and axially oriented ethyl groups constitute the more stable conformations for **7a** and **7a'**, respectively (Table 3 and Scheme 5). In addition, the relative stability for either conformations of **7a** and **7a'** seems to correlate well with the phenyl torsion (ϕ_1) between ring A and the central double bond. Namely, the larger the torsional angle, the higher the energy. Interestingly, in both conformations of **7a** and **7a'** the phenyl torsions between the bottom fragment (ring C) and the central olefin remain es-

entially constant (38.1–39.6°). Apparently, the phenyl torsion- ϕ_1 around the central double bond that can be modulated by the conformation of the DBS plays a pivotal role in the structural stability of the resultant helicene.

As shown in Scheme 5, **7a** preferentially adopts a DBS conformation (**7a_{P-eq}**, $E = 36.0$ kcal/mol) with equatorially disposed ethyl groups. The conformation (**7a_{P-ax}**, $E = 38.3$ kcal/mol) with the flipped DBS ring is clearly less favored (by 2.3 kcal/mol) in view of the larger ϕ_1 (increased by 7.4°) and the increased steric repulsion between the C ring and the proximal axial ethyl group. On the other hand, adoption of the same DBS conformation for **7a'** (**7a'_{M-eq}**, $E = 38.7$ kcal/mol) would impose a larger phenyl distortion for ϕ_1 (-73.5°) by 11.5° beside the steric interaction between ring-C and the proximal axial hydrogen. The unfavorable phenyl and steric strains can be relieved in **7a'_{M-ax}** by a conformational inversion leading to **7a'_{M-ax}** ($E = 34.8$ kcal/mol) in which the ϕ_1 is reduced by almost 18° and the ring C is now anti to the proximal, axial ethyl group. Under such circumstances, the extent of conjugation in **7a'_{M-ax}** becomes slightly better than that in **7a_{P-eq}** as supported by the slight increase in extinction coefficient in the UV spectrum of **7a'**. Therefore, we surmise that **7a_{P-eq}** and **7a'_{M-ax}** are the predominant species in solution (i.e., hexane) for **7a** and **7a'**, respectively. On the basis of this presumption, photoisomerization of **7a_{P-eq}** would involve its initial double bond rotation in a counterclockwise fashion leading to **7a'_{M-eq}** followed by a facile conformational flip leading to **7a'_{M-ax}** (pathway I). Since planarization of the DBS skeleton is a prerequisite step both for the double bond isomerization in the singlet excited states of **7a** and **7a'** and for the conformational flip of the DBS, the intermediacy of **7a'_{M-eq}** (pathway I) for the photoinduced interconversion of **7a_{P-eq}** and **7a'_{M-ax}** might not be necessary. Therefore, an alternative route (pathway II) would involve its double bond isomerization with a concomitant conformational flip of the DBS leading directly to **7a'_{M-ax}**.³⁶ The relative inertness of **7a'_{M-ax}** toward photoisomerization can be rationalized in terms of an increased energy of activation to bring the DBS into planarity by which the torsional angle between ethyl appendages changes from 180° (with 0 strains) to 120° (with two pairs of Et-H torsional and steric strains). On the other hand, to bring the DBS into planarity in the case of **7a_{P-eq}** would involve a torsional angle change from 60° (with one pair of Et-Et gauche strain) to 120°. The eroded switching selectivity at 280 nm along with the improved selectivities at 254 and 310 nm when **7a** was irradiated in cyclohexane suggest that different conformational balances might be involved specifically in this solvent system.

Summary and Conclusions

We have developed C_2 -symmetric DBS-based helicenes as a favorable chirochromic optical switch. The requisite episulfides **6a–c** can be synthesized stereoselectively by coupling of the DBS-derived thioketone **5**, prepared in four steps from the resolved 10,11-bis(hydroxymethyl)-DBS **1**, and the respective in situ-generated diazo compounds. The X-ray structures of all episulfides **6a–c** share a common DBS conformation with equatorially disposed ethyl groups and with the aryl ring in each bottom fragment syn to the proximal equatorial ethyl group. The preferred conformation in the solid state was rationalized in terms of crystal packing effect. Their absolute stereochemistry

(35) (a) Simulations were performed in CAChe Worksystem. (b) The X-ray structure of the corresponding achiral, parent compound was employed as the initial template for the structure construction and minimization of **7a_{P-eq}**.

(36) Photoisomerization with a concomitant conformational flip for 1,1',2,2',3,3',4,4'-octahydro-3,3'-dimethyl-4,4'-biphenanthrylidene as monodirectional molecular rotors has been recently documented, see: Feringa, B. L. *Nature* **1999**, *401*, 152.

is all *S* indicating a predominant approach of the thioketone **5** from the *si* face of the respective diazo compound. Careful examination of the dihedral angles around the central thirrane ring led us to conclude that the steric interaction between ring A and ring C in the episulfide dictates the torsional strain in the central episulfide unit. Reductive desulfurization of (1*R*,1*R*,1'*S*)-episulfides **6a–c** was achieved in a stereospecific manner furnishing respective helicenes **7a–c** of *P* chirality. The X-ray structure of the endo-helicene **7c** reveals a delicate steric match between the DBS conformation and the helicene absolute stereochemistry. The *P* helicene favors, in an energetic sense, the DBS conformation with equatorially oriented ethyl groups. On the opposite, the analogous *M* helicene would prefer an inverted DBS conformation with axial ethyl groups as suggested by molecular simulation.

The helicenes are thermally stable toward epimerization even for the one (**7a**) with the lower fragment derived from α -tetralone. Initial photoisomerization experiments for **7a** performed at 260 and 300 nm allowed us to sort out their irradiation wavelengths (254, 290, and 310 nm) exhibiting distinctive difference in extinction coefficients in the UV difference spectrum before and after experiments. Photoisomerization of **7a** at 254 (or 310) nm and 280 nm led to two pss with opposite diastereoselectivities in four different solvents examined. In all solvents except cyclohexane, the best switching selectivities were attained at 280 nm in a range of 91/9 and 99.6/0.4 (**7a**'/**7a**). The identity of the photoisomerization product **7a**' was secured by the observed isodichroic points in the circular dichroism kinetic experiments, by its thermo-chemical return to **7a**, and by its ¹H NMR spectrum. The photo-inertness of **7b** and **7c** were attributed to their larger deformation between the central olefin and the respective bottom aryl moiety. The high switching selectivity for **7a** at 280 nm in hexane was attributed to a large difference in photoisomerization quantum yields between their interconversion in view of the minor difference in ϵ between both diastereomers. Molecular simulations of the diastereomeric helicenes **7a** and **7a**' with both DBS conformations suggest that the preponderant species of **7a**' in solution adopts a flipped DBS conformation with axial ethyl groups in order to minimize steric encumbrance around the helicity. The sluggish photoresponse of **7a**' in hexane at 280 nm was rationalized in terms of its increased energy of activation toward planarization in its singlet excited-state en-route to a perpendicular singlet excited state.

To our knowledge, our system serves as the best chirochromic optical switch as compared to the examples possessing similar photochromic properties.^{7c,12} A maximum of 133% difference in ϵ and the opposite helicene chirality between these two photostationary states (at 254 and 280 nm) in hexane augur well for its potential application as an optical switch in LC materials. Investigations toward improving the compatibility and the twisting power of our helicene system in common LC phases and toward incorporating a donor–acceptor pair onto the vicinal aryl rings across the central double bond in both dissymmetric triaryl- and tetraaryl-ethylenes are underway.

Experimental Section

General. ¹H NMR and ¹³C NMR were recorded on JEOL JVM-EX400 (400 MHz ¹H, 100 MHz ¹³C) and Varian Gemini-2000 (200 MHz ¹H, 50 MHz ¹³C) spectrometers in deuteriochloroform with tetramethylsilane (TMS) or chloroform as an internal reference unless otherwise stated. Chemical shifts are reported in ppm (δ), coupling constants, *J*, are reported in Hz. Infrared spectra were recorded on a Perkin-Elmer Paragon-500 FTIR spectrometer. Peaks are reported in units of cm^{-1} with the following relative intensities: br (broad), s (strong

67–100%), m (medium 33–67%), or w (weak 0–33%). Mass spectra were recorded on a Finnigan TCQ-700 spectrometer with ionization voltages of 70 eV. Data are reported in the form *m/e* (intensity relative to base = 100%). Combustion analyses were performed on a Perkin-Elmer 2400-CHN analyzer by the Northern Instrument Center of Taiwan. High-resolution mass spectra were recorded on a JEOL JMX-SX/SX 102A spectrometer by the Central Instrument Center of Taiwan. Melting points were determined on a Hargo MP-2D melting point apparatus and are uncorrected. Analytical TLC was performed on Merck silica gel plates with QF-254 indicator. Visualization was accomplished with UV light, PMA, and KMnO₄. Column (flash) chromatography was performed using 32–63 μm silica gel. Solvents for extraction and chromatography were reagent grade. Solvents used for recrystallization were spectral grade and are shown under mp unless otherwise indicated. Analytical high-pressure liquid chromatography (HPLC) was performed on a Jasco Liquid Chromatograph equipped with PU-980 pumps, UV-975 detector, and 807-IT integrator. The columns used were Dical Chiralpak OT and AD columns with the detector wavelength at 254 nm. The flow rate and solvent systems were as denoted. Optical rotation were obtained on a Jasco DIP-1000 Digital Polarimeter at room temperature and reported as follows: $[\alpha]_{\text{wavelength}}$, concentration (*c* = g/100 mL), and solvent. UV–vis spectra were recorded on a HP-8453 Diode Array UV–visible spectrometer in hexane solution unless otherwise noted. Fluorescence spectra were recorded on an Aminco-Browman series-2 Luminescence spectrometer. CD spectra were recorded on a Jasco model J-817 spectropolarimeter. Microscopic analyses were performed with an Olympus BX50-P polarizing microscope equipped with a PM10 automatic photomicrographic system. All reactions were run under nitrogen.

(10*R*,11*R*)-11-([4-Methylphenyl]sulfonyloxy)methyl-10,11-dihydro-5*H*-dibenzo[*a,d*]cycloheptene-10-yl)methyl 4-methyl-1-benzenesulfonate (2). In a 100-mL, three-necked, round-bottomed, flask fitted with a glass stopper, N₂-inlet, and septum was placed diol **1** (1.5053 g, 5.92 mmol) in anhydrous CH₂Cl₂ (55 mL). Anhydrous Et₃N (4.95 mL, 35.5 mmol, 6 equiv) was added at 0 °C followed by addition of *p*-toluenesulfonyl chloride (3.724 g, 19.5 mmol, 3.3 equiv) and 4-(dimethylamino)pyridine (51 mg, 0.41 mmol, 7 mol %) in anhydrous CH₂Cl₂ (18 mL) over 10 min. The resulting reaction mixture was warmed to room temperature and stirred overnight. The reaction mixture was poured into a saturated aqueous NH₄Cl-ice mixture (75 mL, 5/3). The aqueous layer was separated and extracted with CH₂Cl₂ (2 \times 40 mL). The combined organic extracts were washed with saturated aqueous NH₄Cl (25 mL) and H₂O (20 mL), dried (MgSO₄), and evaporated. The crude yellowish solid was purified by column chromatography (hexane/EtOAc, 2/1) to give 3.196 g (96%) of diosylate **2** as a white solid: mp 120.5–121.5 °C (CH₂Cl₂/hexane); ¹H NMR (400 MHz) 7.59 (d, *J* = 8.3, 4H, 4 \times HC(2')), 7.23 (d, *J* = 8.2, 4H, 4 \times HC(3')), 7.15–6.96 (m, 8H, Ar), 4.17 (dd, *J* = 9.9, 5.3, 2H, 2 \times CH₂H₆OTs), 3.97 (s, 2H, H₂C(5)), 3.87 (dd, *J* = 9.8, 8.2, 2H, 2 \times CH₂H₆OTs), 3.52 (quintet, *J* = 5.4, 2H, 2 \times HC(10)), 2.42 (s, 6H, 2 \times CH₃); ¹³C NMR (100 MHz) 144.71 (C(4')), 137.33 (C(4a), C(6a)), 134.02 (C(1a), C(9a)), 132.46 (C(1')), 131.95 (C(4), C(6)), 130.17 (C(2), C(8)), 129.74 (C(3')), 127.66 (C(2')), 127.52 (C(1), C(9)), 126.88 (C(3), C(7)), 70.97 (CH₂OTs), 44.43 (C(10), C(11)), 41.88 (C(5)), 21.57 (CH₃C₆H₄SO₃); IR (CCl₄) 2926 (w), 1717 (m), 1497 (w), 1456 (w), 1372 (s, SO₂, asym.), 1264 (w), 1217 (w), 1190 (s, C–O), 1179 (s, SO₂, sym.), 1097 (w), 968 (m), 818 (s, S–O), 810 (w); MS (70 eV) 390 (M–C₇H₇SO₃H⁺, 11), 219 (24), 218 (100), 217 (28), 205 (40), 204 (14), 203 (27), 202 (12), 192 (13), 191 (21), 179 (10), 178 (22), 172 (14), 92 (58), 65 (11); TLC *R*_f 0.4 (hexane/EtOAc, 2/1); $[\alpha]_{\text{D}} +40.5$ (*c* = 0.74, CH₂Cl₂); Anal. Calcd for C₃₁H₃₀O₆S₂ (562.7): C, 66.17; H, 5.37; S, 11.40. Found: C, 66.14; H, 5.36; S, 11.38.

(10*R*,11*R*)-10,11-Diethyl-10,11-dihydro-5*H*-dibenzo[*a,d*]cycloheptene (3). In a 500 mL, three-necked, round-bottomed, flask equipped with an addition funnel, N₂-inlet, and septum was placed CuI (8.364 g, 43.9 mmol, 6 equiv) suspended in anhydrous ether (37 mL). The reaction flask was cooled on ice and methyllithium (1.6 M in ether, 55 mL, 87.8 mmol, 12 equiv) was added via the addition funnel over 40 min. The solution became clear and yellowish. The resulting (CH₃)₂-CuLi was cannulated to a precooled (–78 °C) solution of diosylate-**2** (4.1187 g, 7.32 mmol) in anhydrous ether (150 mL). The resulting

heterogeneous mixture was gradually warmed to $-10\text{ }^{\circ}\text{C}$ over 1 h and stirred at this temperature for 28 h. Saturated aqueous NH_4Cl (200 mL) was added, and the reaction mixture was warmed to room temperature for 30 min. The aqueous layer was separated and extracted with ether ($3 \times 60\text{ mL}$). The combined organic layers were washed with brine ($2 \times 30\text{ mL}$) and H_2O ($2 \times 20\text{ mL}$), dried (MgSO_4), and evaporated. The crude yellowish oil was purified by column chromatography (hexane/ether, 100/1) to give 1.7995 g (98%) of **3**: bp $125\text{ }^{\circ}\text{C}$ (0.1 Torr); ^1H NMR (400 MHz) 7.22–7.07 (m, 8H, Ar), 4.22 (s, 2H, $\text{H}_2\text{C}(5)$), 2.89 (quintet, $J = 5.5$, 2H, HC(10), HC(11)), 1.66–1.42 (m, 4H, $2 \times \text{CH}_2\text{CH}_3$), 0.86 (t, $J = 7.4$, 6H, $2 \times \text{CH}_2\text{CH}_3$); ^{13}C NMR (100 MHz) 141.30 (C(4a), C(6a)), 137.56 (C(1a), C(9a)), 131.54 (C(4), C(6)), 129.79 (C(2), C(8)), 125.90 (C(1), C(9)), 125.79 (C(3), C(7)), 50.44 (C(10), C(11)), 42.63 (C(5)), 28.08 (CH_2CH_3), 12.63 (CH_2CH_3); IR (neat) 3058 (m), 3017 (m), 2959 (s), 2928 (s), 2870 (s), 1698 (w), 1651 (w), 1557 (w), 1539 (w), 1507 (w), 1491 (s), 1455 (s), 1420 (w), 1375 (m), 1063 (w); MS (70 eV) 250 (M^+ , 32), 222 (11), 221 (56), 207 (10), 191 (16), 180 (16), 179 (100), 178 (37), 165 (10), 91 (24), 43 (41); TLC R_f 0.45 (hexane/ether, 100/1); $[\alpha]_D^{25} +144$ ($c = 0.60$, CH_2Cl_2); Anal. Calcd for $\text{C}_{19}\text{H}_{22}$ (250.4): C, 91.14; H, 8.86. Found: C, 90.98; H, 8.82.

(10R,11R)-10,11-Diethyl-10,11-dihydro-5H-dibenzo[*a,d*]cyclohepten-5-one (4). In a 50-mL, round-bottomed, flask was placed potassium permanganate (77.6 mg, 0.49 mmol, 2.5 equiv) suspended in benzene (6 mL). A solution of dicyclohexano-18-crown-6 (182.53 mg, 0.49 mmol, 2.5 equiv) in benzene (6 mL) was added. The solution became homogeneous and purple. To this mixture was added a solution of 10,11-diethyldibenzosuberane **3** (49.2 mg, 0.20 mmol) in benzene (5 mL). The resulting reaction mixture was stirred at ambient temperature for 2 h and then passed through a silica gel column (20 mm \times 3 cm) using benzene (30 mL) and ether (30 mL) as eluents. The filtrate was concentrated, and the crude oil was purified by column chromatography (hexane/EtOAc, 20/1) to afford 48 mg (92%) of **4** as a yellowish solid: mp $100.5\text{--}101\text{ }^{\circ}\text{C}$ (hexane); ^1H NMR (400 MHz) 8.13 (dd, $J = 8.1$, 1.5, 2H, HC(4), HC(6)), 7.45 (dt, $J = 7.3$, 1.5, 2H, HC(2), HC(8)), 7.34 (dt, $J = 7.8$, 1.2, 2H, HC(3), HC(7)), 7.21 (dd, $J = 7.6$, 1.2, 2H, HC(1), HC(9)), 3.02 (m, 2H, HC(10), HC(11)), 1.55–1.37 (m, 4H, $2 \times \text{CH}_2\text{CH}_3$), 0.84 (t, $J = 7.3$, 6H, $2 \times \text{CH}_2\text{CH}_3$); ^{13}C NMR (100 MHz) 193.55 (C(5)), 143.04 (C(1a), C(9a)), 137.08 (C(4a), C(6a)), 132.31 (C(2), C(8)), 131.34 (C(4), C(6)), 131.28 (C(1), C(9)), 126.57 (C(3), C(7)), 50.99 (C(10), C(11)), 29.59 (CH_2CH_3), 12.48 (CH_2CH_3); IR (CHCl_3) 3068 (m), 3028 (m), 3010 (m), 2964 (s), 2935 (m), 2875 (m), 1639 (s, C=O), 1599 (s, C=C), 1481 (m), 1463 (m), 1454 (m), 1379 (w), 1294 (s), 1226 (m), 1218 (m), 1213 (w), 931 (m); MS (70 eV) 264 (M^+ , 39), 263 (16), 236 (21), 235 (91), 217 (11), 194 (19), 193 (100), 178 (24), 165 (23), 115 (10), 91 (14); TLC R_f 0.45 (hexane/EtOAc, 20/1); $[\alpha]_D^{25} 43.9$ ($c = 0.54$, CH_2Cl_2); Anal. Calcd for $\text{C}_{19}\text{H}_{20}\text{O}$ (264.4): C, 86.32; H, 7.63. Found: C, 86.27; H, 7.64.

(10R,11R)-10,11-Diethyl-10,11-dihydro-5H-dibenzo[*a,d*]cyclohepten-5-thione (5). In a 50-mL, two-necked, round-bottomed, flask was placed P_4S_{10} (444.5 mg, 1 mmol, 4.0 equiv) suspended in anhydrous toluene (5 mL). To the reaction flask was added a solution of **4** (264 mg, 1 mmol) in anhydrous toluene (10 mL). The resulting reaction mixture was stirred at $100\text{ }^{\circ}\text{C}$ for 15 h and then passed through a short column of neutral alumina (15 mm \times 5 cm) using *n*-hexane as eluent. The filtrate was collected and concentrated to give 280 mg (100%) of **5** as a blue oil: ^1H NMR (200 MHz, CDCl_3) 7.93 (dd, $J = 7.8$, 1.4, 2H, HC(4), HC(6)), 7.41–7.06 (m, 6H, Ar), 2.96 (q, $J = 6.2$, 2H, HC(10), HC(11)), 1.65–1.40 (m, 4H, $2 \times \text{CH}_2\text{CH}_3$), 0.86 (t, $J = 7.6$, 6H, $2 \times \text{CH}_2\text{CH}_3$); TLC R_f 0.32 (hexane).

(10R,11R,1'S)-10,11-Diethyl-5-(1,2,3,4-tetrahydro-1-naphthalenylidene-2'-thirrane)-10,11-dihydro-5H-dibenzo[*a,d*]cycloheptene (6a). In a 50-mL, two-necked, round-bottomed, flask fitted with a Schlenk filtration tube and septum was placed hydrazone (272 mg, 1.7 mmol) in anhydrous CH_2Cl_2 (10 mL). The solution was cooled to $-30\text{ }^{\circ}\text{C}$, whereupon MgSO_4 (1.11 g), Ag_2O (588 mg, 2.55 mmol, 1.5 equiv), and a saturated solution of KOH in methanol (1.33 mL) were successively added. After having been stirred for 40 min, the resulting deep red solution was filtered into another ice-cooled flask, and the remaining residue was washed with CH_2Cl_2 (5 mL). To this clear solution was added dropwise a solution of thioiketone **5** (1.0 M in

CH_2Cl_2) by microsyringe. Evolution of nitrogen was observed, and the deep red solution slowly decolorized. The thioiketone was added until the evolution of nitrogen had subsided. A total of 204 mg (0.72 mmol) of **5** was added. After having been stirred for 16 h, the resulting reaction mixture was quenched by saturated aqueous NaHCO_3 (15 mL). The aqueous layer was separated and extracted with ether ($3 \times 15\text{ mL}$). The combined organic layers were dried (MgSO_4), filtered, and evaporated. The bluish residue was purified by column chromatography (hexane) to get 140 mg (47%) of **6a** as a white solid: mp $154\text{--}156\text{ }^{\circ}\text{C}$ (hexane); ^1H NMR (400 MHz, CDCl_3) 8.01–7.96 (m, 1H, HC(4)), 7.46 (dd, $J = 7.2$, 1.4, 1H, HC(6)), 7.24–7.18 (m, 2H, HC(5'), HC(8')), 7.12–6.96 (m, 6H, Ar), 6.81 (t, $J = 8.0$, 1H, HC(2)), 6.70 (t, $J = 8.0$, 1H, HC(8)), 3.17–3.03 (m, 1H, $\text{H}_{\text{eq}}\text{C}(4')$), 2.90–2.82 (m, 2H, $\text{H}_{\text{ax}}\text{C}(4')$, HC(10)), 2.42–2.28 (m, 2H, $\text{H}_{\text{eq}}\text{C}(2')$, HC(11)), 2.04–1.81 (m, 5H, $\text{H}_2\text{C}(3')$, $\text{H}_2\text{C}(12)$, $\text{H}_{\text{ax}}\text{C}(2')$), 1.54–1.41 (m, 1H, $\text{H}_a\text{H}_b\text{C}(13)\text{CH}_3$), 1.03 (t, $J = 7.4$, 3H, $\text{H}_3\text{C}(14)$), 0.64–0.44 (m, 1H, $\text{H}_a\text{H}_b\text{C}(13)\text{CH}_3$), 0.32 (t, $J = 7.4$, 3H, $\text{H}_3\text{C}(15)$); ^{13}C NMR (100 MHz, CDCl_3) 145.83 (C(4a)), 140.62 (C(6a)), 139.56 (C(1a)), 138.37 (C(9a)), 136.93 (C(8'a)), 136.57 (C(4'a)), 131.92 (C(1)), 128.81 (C(9)), 128.79 (C(5')), 128.72 (C(6')), 127.87 (C(7')), 127.27 (C(2)), 126.99 (C(8)), 126.71 (C(3)), 125.91 (C(7)), 125.81 (C(4)), 125.62 (C(6)), 125.32 (C(8')), 71.57 (C(1')), 58.60 (C(5)), 51.72 (C(10)), 44.15 (C(11)), 39.74 (C(2')), 31.42 (C(4')), 29.50 (C(3')), 23.04 (C(12)), 22.41 (C(13)), 12.67 (C(14)), 11.51 (C(15)); IR (CCl_4) 2958 (m), 2929 (m), 2871 (m), 2289 (w), 1731 (m), 1550 (s), 1457 (w), 1376 (w), 1253 (m), 1218 (m), 1115 (w), 1070 (w), 1005 (m), 979 (m), 784 (s); MS (70 eV) 411 (27), 410 (M^+ , 100), 381 (33), 347 (42), 326 (52), 305 (56), 303 (13), 247 (30), 219 (63), 178 (55), 165 (11), 129 (33), 91 (25); TLC R_f 0.42 (hexane); $[\lambda]_D^{25} -30$ ($c = 0.03$, *i*-PrOH); Anal. Calcd For $\text{C}_{29}\text{H}_{30}\text{S}$ (410.6): C, 84.93; H, 7.36. Found: C, 85.21; H, 7.03.

(10R,11R,1'S)-10,11-Diethyl-5-(1,2,3,4-tetrahydro-1-phenanthrenylidene-2'-thirrane)-10,11-dihydro-5H-dibenzo[*a,d*]cycloheptene (6b). In a 50-mL, two-necked, round-bottomed, flask fitted with a Schlenk filtration tube and septum was placed hydrazone (315 mg, 1.5 mmol) in anhydrous CH_2Cl_2 (10 mL). The solution was cooled to $-30\text{ }^{\circ}\text{C}$, whereupon MgSO_4 (0.98 g), Ag_2O (518 mg, 2.25 mmol, 1.5 equiv), and a saturated solution of KOH in methanol (1.18 mL) were successively added. After having been stirred for 40 min, the resulting deep red solution was filtered into another ice-cooled flask, and the remaining residue was washed with CH_2Cl_2 (5 mL). To this clear solution was added dropwise a solution of thioiketone **5** (1.0 M in CH_2Cl_2) by microsyringe. Evolution of nitrogen was observed, and the deep red solution slowly decolorized. The thioiketone was added until the evolution of nitrogen had subsided. A total of 188 mg (0.67 mmol) of **5** was added. After having been stirred for 16 h, the resulting reaction mixture was quenched by saturated aqueous NaHCO_3 (15 mL). The aqueous layer was separated and extracted with ether ($3 \times 15\text{ mL}$). The combined organic layers were dried (MgSO_4), filtered, and evaporated. The bluish residue was purified by column chromatography (hexane) to get 139 mg (45%) of **6b** as a white solid: mp $188\text{--}190\text{ }^{\circ}\text{C}$ (hexane); ^1H NMR (400 MHz, CDCl_3) 8.14 (dd, $J = 8.0$, 4.0, 1H, HC(5')), 8.09 (d, $J = 8.0$, 1H, HC(8')), 7.69 (d, $J = 8.0$, 1H, HC(1)), 7.58–7.54 (m, 2H, HC(9'), HC(8')), 7.50–7.46 (m, 1H, HC(6')), 7.32–7.15 (m, 7H, Ar), 6.87 (d, $J = 8.0$, 1H, HC(10')), 3.56 (dt, $J = 8.0$, 4.0, 1H, $\text{H}_{\text{eq}}\text{C}(4')$), 3.19–3.09 (m, 2H, $\text{H}_a\text{H}_b\text{C}(4)$, HC(10)), 2.56 (td, $J = 8.0$, 4.0, 1H, $\text{H}_{\text{ax}}\text{C}(2')$), 2.36 (td, $J = 8.0$, 4.0, 1H, HC(11)), 2.23–2.10 (m, 2H, $\text{H}_a\text{H}_b\text{C}(12)$, $\text{H}_{\text{eq}}\text{C}(2')$), 2.03–1.95 (m, 3H, $\text{H}_2\text{C}(3')$, $\text{H}_a\text{H}_b\text{C}(12)$), 1.44–1.38 (m, 1H, $\text{H}_a\text{H}_b\text{C}(13)$), 1.10 (t, 3H, $J = 8.0$, $\text{H}_3\text{C}(14)$), 0.52–0.45 (m, 1H, $\text{H}_a\text{H}_b\text{C}(13)$), 0.23 (t, 3H, $J = 8.0$, $\text{H}_3\text{C}(15)$); ^{13}C NMR (100 MHz, CDCl_3) 146.02 (C(6a)), 140.53 (C(4a)), 138.59 (C(9a)), 136.97 (C(1a)), 135.43 (C(10'a)), 134.14 (C(4'a)), 132.20 (C(4'ab)), 132.02 (C(8'a)), 131.92 (C(1)), 131.75 (C(9)), 127.99 (C(9')), 127.82 (C(6')), 127.27 (C(7')), 126.99 (C(8')), 126.03 (C(2)), 126.00 (C(8)), 125.93 (C(3)), 125.80 (C(7)), 125.63 (C(5')), 25.50 (C(4)), 125.04 (C(6)), 123.33 (C(10')), 71.54 (C(1')), 60.18 (C(5)), 51.76 (C(10)), 44.24 (C(11)), 39.01 (C(2')), 29.39 (C(4')), 27.17 (C(12)), 23.02 (C(13)), 22.07 (C(3')), 12.76 (C(14)), 11.34 (C(15)); IR (CCl_4) 2929 (m), 2292 (w), 1733 (w), 1684 (w), 1653 (w), 1550 (s), 1253 (m), 1218 (m), 1110 (w), 1070 (w), 1006 (m), 979 (m); MS (70 eV) 460 (M^+ , 34), 428 (28), 399 (40), 355 (13), 305 (13), 265 (14), 247 (100), 219 (45), 178 (51), 141 (29), 91 (14); TLC R_f 0.33 (hexane); $[\lambda]_D^{25} -43$ (c

= 0.03, *i*-PrOH); Anal. Calcd For C₃₃H₃₂S (460.68): C, 86.04; H, 7.00. Found: C, 85.56; H, 6.72.

(10R,11R,1'S)-10,11-Diethyl-5-(1,2,3,4-tetrahydro-4-phenanthrenylidene-2-thiirane)-10,11-dihydro-5H-dibenzo[*a,d*]cycloheptene (6c). In a 50-mL, two-necked, round-bottomed, flask fitted with a Schlenk filtration tube and septum was placed hydrazone (420 mg, 2.0 mmol) in anhydrous CH₂Cl₂ (10 mL). The solution was cooled to -30 °C, whereupon MgSO₄ (1.30 g), Ag₂O (691 mg, 3.0 mmol, 1.5 equiv), and a saturated solution of KOH in methanol (1.57 mL) were successively added. After having been stirred for 40 min, the resulting deep red solution was filtered into another ice-cooled flask, and the remaining residue was washed with CH₂Cl₂ (5 mL). To this clear solution was added dropwise a solution of thioketone **5** (1.0 M in CH₂Cl₂) by microsyringe. Evolution of nitrogen was observed, and the deep red solution slowly decolorized. The thioketone was added until the evolution of nitrogen had subsided. A total of 224 mg (0.8 mmol) of **5** was added. After having been stirred for 16 h, the resulting reaction mixture was quenched by saturated aqueous NaHCO₃ (15 mL). The aqueous layer was separated and extracted with ether (3 × 15 mL). The combined organic layers were dried (MgSO₄), filtered, and evaporated. The bluish residue was purified by column chromatography (hexane) to get 126 mg (34%) of **6c** as a white solid: mp 154–156 °C (hexane); ¹H NMR (400 MHz, CDCl₃) 9.17 (d, *J* = 8.0, 1H, HC(10')), 8.08 (d, *J* = 8.0, 1H, HC(7')), 7.66 (d, *J* = 8.0, 1H, HC(6')), 7.62 (d, *J* = 8.0, 1H, HC(8')), 7.57 (d, *J* = 8.0, 1H, HC(6)), 7.37–7.12 (m, 6H, Ar), 6.97 (t, *J* = 8.0, 1H, HC(2)), 6.78 (t, *J* = 8.0, 1H, HC(8)), 6.47 (d, *J* = 8.0, 1H, HC(1)), 3.24 (td, *J* = 8.0, 4.0, 1H, HC(10)), 3.21–3.12 (m, 1H, H_aH_bC(4')), 2.88 (m, 1H, H_aH_bC(4')), 2.48 (td, *J* = 8.0, 4.0, 1H, H_{ax}C(2')), 2.14–1.95 (m, 5H, H₂C(3'), H_{eq}C(2'), HC(11)), 1.69–1.51 (m, 1H, H_aH_bC(12)), 1.22–1.08 (m, 1H, H_aH_bC(12)), 1.10 (t, *J* = 8.0, 3H, H₃C(14)), 1.02–0.94 (m, 1H, H_aH_bC(13)), 0.03 (t, *J* = 8.0, 3H, H₃C(15)), -0.69–-0.80 (m, 1H, H_aH_bC(13)); ¹³C NMR (100 MHz, CDCl₃) 147.25 (C(4a)), 141.48 (C(6a)), 139.44 (C(10'a)), 138.59 (C(6'a)), 136.29 (C(9a)), 133.34 (C(1a)), 133.08 (C(4'a)), 131.78 (C(10'ab)), 129.77 (C(9)), 128.63 (C(1)), 128.14 (C(5')), 127.99 (C(2)), 126.91 (C(8)), 126.83 (C(9')), 126.74 (C(8')), 126.55 (C(7')), 126.41 (C(6')), 126.00 (C(7)), 125.83 (C(3)), 125.23 (C(10')), 124.29 (C(4)), 123.10 (C(6)), 71.35 (C(1')), 60.31 (C(5)), 51.77 (C(10)), 46.65 (C(11)), 45.35 (C(2')), 34.15 (C(4')), 28.39 (C(12)), 23.25 (C(13)), 21.16 (C(3')), 12.93 (C(14)), 12.74 (C(15)); IR (CCl₄) 2291 (w), 1550 (s), 1253 (m), 1218 (m), 1108 (w), 1068 (w), 1006 (m), 979 (m), 810 (s); MS (70 eV) 460 (M⁺, 100), 428 (26), 397 (10), 355 (12), 318 (10), 305 (26), 247 (24), 221 (15), 191 (19), 179 (52), 141 (36), 91 (14); TLC: *R*_f 0.32 (hexane); [λ]_D -48 (*c* = 0.06, *i*-PrOH); Anal. Calcd For C₃₃H₃₂S (460.68): C, 86.04; H, 7.00. Found: C, 86.01; H, 7.29.

(10R,11R,P)-10,11-Diethyl-5-(1,2,3,4-tetrahydro-1-naphthalenylidene)-10,11-dihydro-5H-dibenzo[*a,d*]cycloheptene (7a). In a 25-mL, two-necked, round-bottomed, flask fitted with a condenser topped with an N₂-inlet and septum was placed episulfide **6a** (54 mg, 0.13 mmol) and copper powder (84 mg, 1.3 mmol, 10 equiv) in anhydrous xylene (5 mL). The resulting reaction mixture was refluxed for 2 h and then quenched with saturated aqueous NaHCO₃ (5 mL). The aqueous layer was separated and extracted with ether (3 × 15 mL). The combined organic layers were dried (MgSO₄), filtered, and evaporated. The crude oil was purified by column chromatography (hexane) to get 49 mg (100%) of **7a** as a colorless oil: ¹H NMR (400 MHz, CDCl₃) 7.19–7.08 (m, 5H, Ar), 7.06–7.01 (m, 3H, Ar), 6.88 (t, *J* = 8.0, 1H, HC(2)), 6.82 (d, *J* = 8.0, 1H, HC(6)), 6.79–6.71 (m, 2H, HC(4), HC(8')), 3.30–3.22 (m, 1H, HC(11)), 3.08–2.91 (m, 3H, H₂C(4'), H_{ax}C(2'), H₂C(1'), HC(11)), 2.78–2.72 (m, 1H, HC(10)), 2.13–1.73 (m, 5H, H_{eq}C(2'), H₂C(13), H₂C(3')), 1.65–1.51 (m, 1H, H_aH_bC(12)), 1.48–1.35 (m, 1H, H_aH_bC(12)), 1.06 (t, *J* = 8.0, 3H, H₃C(15)), 0.78 (t, 3H, *J* = 8.0, H₃C(14)); ¹³C NMR (100 MHz, CDCl₃) 144.72 (C(5)), 142.27 (C(1')), 140.62 (C(1a)), 139.07 (C(9a)), 138.85 (C(1'a)), 136.64 (C(4'a)), 131.69 (C(4)), 131.32 (C(6)), 128.69 (C(4)), 128.53 (C(1)), 127.76 (C(9)), 127.48 (C(7')), 127.26 (C(5')), 126.38 (C(6')), 126.35 (C(8')), 126.32 (C(6a)), 126.27 (C(2)), 126.19 (C(8)), 125.28 (C(3)), 124.36 (C(7)), 50.59 (C(11)), 46.01 (C(10)), 29.96 (C(4')), 29.00 (C(2')), 28.96 (C(13)), 25.57 (C(12)), 23.99 (C(3')), 12.96 (C(15)), 10.49 (C(14)); IR (CCl₄) 2929 (m), 2918 (m), 2890 (m), 1754

(m), 1450 (w), 1353 (w), 1240 (w), 1070 (w), 770 (s); MS (70 eV) 378 (M⁺, 100), 349 (67), 289 (16), 247 (46), 219 (33), 190 (25), 145 (10); High-resolution MS calcd for C₂₉H₃₀: 378.2347, found: 378.2345; TLC *R*_f 0.38 (hexane); [λ]_D +62 (*c* = 0.1, *i*-PrOH); HPLC *t*_R 8.87 min (Chiralpak OT, *i*-PrOH/hexane, 10/90, -20 °C, 0.5 mL/min, λ = 254 nm).

(10R,11R,P)-10,11-Diethyl-5-(1,2,3,4-tetrahydro-1-phenanthrenylidene)-10,11-dihydro-5H-dibenzo[*a,d*] cycloheptene (7b). In a 25-mL, two-necked, round-bottomed, flask fitted with a condenser topped with an N₂-inlet and septum was placed episulfide **6b** (82 mg, 0.18 mmol) and copper powder (115 mg, 1.8 mmol, 10 equiv) in anhydrous xylene (0.5 mL). The resulting reaction mixture was refluxed for 2 h and then quenched with saturated aqueous NaHCO₃ (5 mL). The aqueous layer was separated and extracted with ether (3 × 15 mL). The combined organic layers were dried (MgSO₄), filtered, and evaporated. The crude oil was purified by column chromatography (hexane) to get 45 mg (58%) of **7b** as a white solid: ¹H NMR (400 MHz, CDCl₃) 8.04 (d, 1H, *J* = 8.0, HC(8')), 7.65 (d, 1H, *J* = 8.0, HC(5')), 7.52–7.36 (m, 2H, Ar), 7.28–7.00 (m, 6H, Ar), 6.84–6.80 (m, 4H, HC(2), HC(4), HC(6), HC(8')), 3.60–3.15 (m, 4H, HC(11), H_aH_bC(4'), H_{ax}C(2'), HC(10)), 2.82–2.63 (m, 1H, H_aH_bC(4')), 2.30–1.72 (m, 5H, H_{eq}C(2'), H₂C(3'), H₂C(12)), 1.23–0.75 (m, 2H, H₂C(12)), 1.08 (t, *J* = 8.0, 3H, H₃C(15)), 0.80 (t, *J* = 8.0, 3H, H₃C(14)); ¹³C NMR (50 MHz, CDCl₃) 144.23 (C(5)), 142.45 (C(1')), 140.62 (C(6a)), 139.57 (C(4a)), 136.55 (C(9a)), 134.53 (C(1a)), 133.65 (C(10'a)), 133.30 (C(4'a)), 131.45 (C(4'ab)), 128.33 (C(8'a)), 128.27 (C(1)), 128.15 (C(9)), 127.99 (C(9')), 127.07 (C(6')), 126.63 (C(7')), 126.45 (C(8')), 126.37 (C(2)), 125.87 (C(8)), 125.82 (C(3)), 125.67 (C(7)), 125.51 (C(5')), 125.45 (C(4)), 124.31 (C(6)), 123.47 (C(10')), 50.42 (C(11)), 46.38 (C(10)), 28.92 (C(12)), 28.66 (C(13)), 26.42 (C(2')), 26.05 (C(4')), 24.35 (C(3')), 12.85 (C(15)), 10.47 (C(14)); IR (CCl₄) 3065 (w), 3018 (w), 2965 (m), 2931 (m), 2874 (w), 1598 (w), 1509 (w), 1480 (w), 1462 (w), 1379 (w), 1191 (w), 1105 (w), 1030 (w); TLC *R*_f 0.31 (hexane); [λ]_D +83 (*c* = 0.03, *i*-PrOH); Anal. Calcd For C₃₃H₃₂ (428.6): C, 92.47; H, 7.53. Found: C, 92.22; H, 7.59.

(10R,11R,P)-10,11-Diethyl-5-(1,2,3,4-tetrahydro-4-phenanthrenylidene)-10,11-dihydro-5H-dibenzo[*a,d*]cycloheptene (7c). In a 25-mL, two-necked, round-bottomed, flask fitted with a condenser topped with an N₂-inlet and septum was placed episulfide **6c** (20 mg, 0.04 mmol) and copper powder (28 mg, 0.4 mmol, 10 equiv) in anhydrous xylene (0.5 mL). The resulting reaction mixture was refluxed for 2 h and then quenched with saturated aqueous NaHCO₃ (5 mL). The aqueous layer was separated and extracted with ether (3 × 15 mL). The combined organic layers were dried (MgSO₄), filtered, and evaporated. The crude oil was purified by column chromatography (hexane) to get 18 mg (98%) of **7c** as a white solid: mp 142–146 °C (hexane); ¹H NMR (400 MHz, CDCl₃) 7.75–7.64 (m, 2H, HC(6'), HC(7')), 7.59 (d, *J* = 8.0, 1H, HC(5')), 7.38 (d, *J* = 8.0, 1H, HC(10')), 7.28–6.95 (m, 6H, Ar), 6.77 (t, *J* = 8.0, 1H, HC(2)), 6.31 (t, *J* = 8.0, 1H, HC(3)), 6.23 (d, *J* = 8.0, 1H, HC(4)), 3.49 (m, 1H, HC(11)), 3.12–2.83 (m, 4H, H₂C(4), HC(10), H_{eq}C(2')), 2.49–2.35 (m, 1H, H_aH_bC(13)), 2.33–1.61 (m, 6H, H_aH_bC(13), H_{ax}C(2'), H₂C(3'), H₂C(12)), 1.13 (t, *J* = 8.0, 3H, H₃C(15)), 0.98 (t, *J* = 8.0, H₃C(14)); ¹³C NMR (100 MHz, CDCl₃) 142.80 (C(5)), 142.45 (C(1')), 141.87 (C(1a)), 140.41 (C(9a)), 139.66 (C(6'a)), 138.16 (C(4'a)), 134.83 (C(10'a)), 132.90 (C(10'ab)), 132.07 (C(4)), 130.99 (C(6)), 129.67 (C(4a)), 129.21 (C(1)), 128.37 (C(9)), 128.19 (C(3)), 127.52 (C(8')), 127.36 (C(7')), 126.99 (C(6a)), 126.81 (C(5')), 126.73 (C(6')), 126.17 (C(10')), 126.07 (C(2)), 125.24 (C(8)), 124.67 (C(3)), 124.07 (C(7)), 50.81 (C(11)), 45.81 (C(10)), 29.10 (C(4')), 28.51 (C(13)), 28.87 (C(2')), 26.90 (C(12)), 21.55 (C(3')), 12.36 (C(15)), 10.01 (C(14)); IR (CCl₄) 2293 (m), 1550 (s), 1253 (m), 1218 (m), 1108 (w), 1068 (w), 1006 (m), 979 (m), 774 (s); MS (70 eV) 428 (M⁺, 23), 247 (38), 229 (16), 219 (100), 203 (50), 200 (22); [λ]_D -82 (*c* = 0.08, *i*-PrOH); TLC *R*_f 0.35 (hexane); Anal. Calcd For C₃₃H₃₂ (428.6): C, 92.47; H, 7.53. Found: C, 92.40; H, 7.53.

(10R,11R,M)-10,11-Diethyl-5-(1,2,3,4-tetrahydro-1-naphthalenylidene)-10,11-dihydro-5H-dibenzo[*a,d*]cycloheptene (7a'). A solution of **7a** (3.5 mg, 9.2 μmol) in degassed hexane (0.5 mL) was irradiated with 300 W Xe-lamp equipped with a monochromator. The irradiation wavelength was 280 nm with a slit size equivalent to 16 nm bandwidth.

The experiment was carried on for 4 days till a constant composition (99.6/0.4, **7a'**/**7a**) was observed by HPLC analysis on Chiralpak OT column. The solution was concentrated to give **7a'** quantitatively as a white solid: ^1H NMR (200 MHz, CDCl_3) 8.57 (t, $J = 10.0$, 1H, HC(3)), 7.46 (t, $J = 10.2$, 1H, HC(7')), 7.37 (t, $J = 6.8$, 1H, HC(6')), 7.27–7.01 (m, 9H, Ar), 3.21–2.71 (m, 7H, HC(11), HC(10), $\text{H}_2\text{C}(4')$, $\text{H}_{\text{ax}}\text{C}(2')$, $\text{H}_2\text{C}(12)$), 2.16–1.78 (m, 5H, $\text{H}_{\text{eq}}\text{C}(2')$, $\text{H}_2\text{C}(13)$, $\text{H}_2\text{C}(3')$), 0.89 (t, $J = 6.2$, 3H, $\text{H}_3\text{C}(14)$), 0.83 (t, 3H, $J = 7.4$, $\text{H}_3\text{C}(15)$); ^{13}C NMR (100 MHz, CDCl_3) 142.31 (C(5)), 141.18 (C(1a)), 139.53 (C(9a)), 138.21 (C(7'a)), 137.44 (C(8')), 135.36 (C(4'a)), 133.99 (C(4)), 133.83 (C(6)), 132.47 (C(1)), 130.75 (C(9)), 130.42 (C(6')), 127.56 (C(4')), 127.34 (C(5')), 126.85 (C(7')), 126.45 (C(4a)), 125.96 (C(6a)), 125.36 (C(2)), 124.73 (C(8)), 121.79 (C(3)), 121.34 (C(7)), 53.99 (C(11)), 49.56 (C(10)), 32.18 (C(13)), 31.05 (C(12)), 24.03 (C(1')), 23.20 (C(3')), 21.99 (C(2')), 12.24 (C(15)), 11.80 (C(14)); MS (70 eV) 378 (M^+ , 7), 377 (24), 376 (92), 347 (45), 305 (100), 289 (24), 276 (11), 239 (7), 194 (7), 167 (8), 145 (11); High-Resolution MS calcd for $\text{C}_{29}\text{H}_{30}$: 378.2347, found: 378.2342; TLC R_f 0.38 (hexane); $[\alpha]_{\text{D}}^{+55}$ ($c = 0.01$, *i*-PrOH); HPLC t_{R} 10.40 min (Chiralpak OT, *i*-PrOH/hexane, 10/90, -20 °C, 0.5 mL/min, $\lambda = 254$ nm).

Acknowledgment. We are indebted to Professor I-Jy Chang for helpful discussion on the photophysical aspects of our helicenes and Professor Chong-Mou Wang for the generous sharing of his photochemistry equipment with us. We thank Professor Chuen-Her Ueng and Professor Yu Wang for X-ray crystallographic analyses of **6a–c** and **7c**. We are grateful to the National Science Council of the Republic of China for a generous support of this research.

Supporting Information Available: X-ray position parameters, full bond distances and angles, and ORTEP drawings for **6a–c** and **7c** as well as chemical equations and numberings of products in the Experimental Section are included (PDF). This material is available free of charge via the Internet at <http://pubs.acs.org>.

JA993297D